

DESY 95-079, hep-ex/yymmnn
April 1995

**Leptoquarks and Compositeness Scales
from a Contact Interaction Analysis of
Deep Inelastic $e^\pm p$ Scattering at HERA**

H1 Collaboration

arXiv:hep-ex/9504008v1 21 Apr 1995

ISSN 0418-9833

Leptoquarks and Compositeness Scales from a Contact Interaction Analysis of Deep Inelastic $e^\pm p$ Scattering at HERA

H1 Collaboration

Abstract. A contact interaction analysis is presented to search for new phenomena beyond the Standard Model in deep inelastic $e^\pm p \rightarrow e^\pm \text{hadrons}$ scattering. The data are collected with the H1 detector at HERA and correspond to integrated luminosities of 0.909 pb^{-1} and 2.947 pb^{-1} for electron and positron beams, respectively. The differential cross sections $d\sigma/dQ^2$ are measured in the Q^2 range between 160 GeV^2 and $20,000 \text{ GeV}^2$. The absence of any significant deviation from the Standard Model prediction is used to constrain the couplings and masses of new leptoquarks and to set limits on electron–quark compositeness scales and on the radius of light quarks.

S. Aid¹³, V. Andreev²⁵, B. Andrieu²⁸, R.-D. Appuhn¹¹, M. Arpagaus³⁶, A. Babaev²⁴,
 J. Bähr³⁵, J. Bán¹⁷, Y. Ban²⁷, P. Baranov²⁵, E. Barrelet²⁹, R. Barschke¹¹, W. Bartel¹¹,
 M. Barth⁴, U. Bassler²⁹, H.P. Beck³⁷, H.-J. Behrend¹¹, A. Belousov²⁵, Ch. Berger¹,
 G. Bernardi²⁹, R. Bernet³⁶, G. Bertrand-Coremans⁴, M. Besançon⁹, R. Beyer¹¹,
 P. Biddulph²², P. Bispham²², J.C. Bizot²⁷, V. Blobel¹³, K. Borrás⁸, F. Botterweck⁴,
 V. Boudry⁷, A. Braemer¹⁴, F. Brasse¹¹, W. Braunschweig¹, V. Brisson²⁷, D. Bruncko¹⁷,
 C. Brune¹⁵, R. Buchholz¹¹, L. Büngener¹³, J. Bürger¹¹, F.W. Büsler¹³, A. Buniatian^{11,38},
 S. Burke¹⁸, M.J. Burton²², G. Buschhorn²⁶, A.J. Campbell¹¹, T. Carli²⁶, F. Charles¹¹,
 M. Charlet¹¹, D. Clarke⁵, A.B. Clegg¹⁸, B. Clerbaux⁴, J.G. Contreras⁸, C. Cormack¹⁹,
 J.A. Coughlan⁵, A. Courau²⁷, Ch. Coutures⁹, G. Cozzika⁹, L. Criegee¹¹, D.G. Cussans⁵,
 J. Cvach³⁰, S. Dagoret²⁹, J.B. Dainton¹⁹, W.D. Dau¹⁶, K. Daum³⁴, M. David⁹, B. Delcourt²⁷,
 L. Del Buono²⁹, A. De Roeck¹¹, E.A. De Wolf⁴, P. Di Nezza³², C. Dollfus³⁷, J.D. Dowell³,
 H.B. Dreis², A. Droutskoi²⁴, J. Duboc²⁹, D. Düllmann¹³, O. Dünger¹³, H. Duhm¹², J. Ebert³⁴,
 T.R. Ebert¹⁹, G. Eckerlin¹¹, V. Efremenko²⁴, S. Egli³⁷, H. Ehrlichmann³⁵, S. Eichenberger³⁷,
 R. Eichler³⁶, F. Eisele¹⁴, E. Eisenhandler²⁰, R.J. Ellison²², E. Elsen¹¹, M. Erdmann¹⁴,
 W. Erdmann³⁶, E. Evrard⁴, L. Favart⁴, A. Fedotov²⁴, D. Feeken¹³, R. Felst¹¹, J. Feltesse⁹,
 J. Ferencei¹⁵, F. Ferrarotto³², K. Flamm¹¹, M. Fleischer²⁶, M. Flieser²⁶, G. Flügge²,
 A. Fomenko²⁵, B. Fominykh²⁴, M. Forbush⁷, J. Formánek³¹, J.M. Foster²², G. Franke¹¹,
 E. Fretwurst¹², E. Gabathuler¹⁹, K. Gabathuler³³, J. Garvey³, J. Gayler¹¹, M. Gebauer⁸,
 A. Gellrich¹¹, H. Genzel¹, R. Gerhards¹¹, A. Glazov³⁵, U. Goerlach¹¹, L. Goerlich⁶,
 N. Gogitidze²⁵, M. Goldberg²⁹, D. Goldner⁸, B. Gonzalez-Pineiro²⁹, I. Gorelov²⁴,
 P. Goritchev²⁴, C. Grab³⁶, H. Grässler², R. Grässler², T. Greenshaw¹⁹, G. Grindhammer²⁶,
 A. Gruber²⁶, C. Gruber¹⁶, J. Haack³⁵, D. Haidt¹¹, L. Hajduk⁶, O. Hamon²⁹, M. Hampel¹,
 M. Hapke¹¹, W.J. Haynes⁵, J. Heatherington²⁰, G. Heinzelmann¹³, R.C.W. Henderson¹⁸,
 H. Henschel³⁵, I. Herynek³⁰, M.F. Hess²⁶, W. Hildesheim¹¹, P. Hill⁵, K.H. Hiller³⁵,
 C.D. Hilton²², J. Hladký³⁰, K.C. Hoeger²², M. Höppner⁸, R. Horisberger³³, V.L. Hudgson³,
 Ph. Huet⁴, M. Hütte⁸, H. Hufnagel¹⁴, M. Ibbotson²², H. Itterbeck¹, M.-A. Jabiol⁹,
 A. Jacholkowska²⁷, C. Jacobsson²¹, M. Jaffre²⁷, J. Janoth¹⁵, T. Jansen¹¹, L. Jönsson²¹,
 D.P. Johnson⁴, L. Johnson¹⁸, H. Jung²⁹, P.I.P. Kalmus²⁰, D. Kant²⁰, R. Kaschowitz²,
 P. Kassermann¹², U. Kathage¹⁶, J. Katzy¹⁴, H.H. Kaufmann³⁵, S. Kazarian¹¹, I.R. Kenyon³,
 S. Kermiche²³, C. Keuker¹, C. Kiesling²⁶, M. Klein³⁵, C. Kleinwort¹³, G. Knies¹¹, W. Ko⁷,
 T. Köhler¹, J.H. Köhne²⁶, H. Kolanoski⁸, F. Kole⁷, S.D. Kolya²², V. Korbel¹¹, M. Korn⁸,
 P. Kostka³⁵, S.K. Kotelnikov²⁵, T. Krämerkämper⁸, M.W. Krasny^{6,29}, H. Krehbiel¹¹,
 D. Krücker², U. Krüger¹¹, U. Krüner-Marquis¹¹, H. Küster², M. Kuhlen²⁶, T. Kurča¹⁷,
 J. Kurzhöfer⁸, B. Kuznik³⁴, D. Lacour²⁹, F. Lamarche²⁸, R. Lander⁷, M.P.J. Landon²⁰,
 W. Lange³⁵, P. Lanius²⁶, J.-F. Laporte⁹, A. Lebedev²⁵, F. Lehner¹¹, C. Leverenz¹¹,
 S. Levonian²⁵, Ch. Ley², G. Lindström¹², J. Link⁷, F. Linsel¹¹, J. Lipinski¹³, B. List¹¹,
 G. Lobo²⁷, P. Loch²⁷, H. Lohmander²¹, J.W. Lomas²², G.C. Lopez²⁰, V. Lubimov²⁴,
 D. Lüke^{8,11}, N. Magnussen³⁴, E. Malinovski²⁵, S. Mani⁷, R. Maraček¹⁷, P. Marage⁴,
 J. Marks²³, R. Marshall²², J. Martens³⁴, G. Martin¹³, R. Martin¹¹, H.-U. Martyn¹,
 J. Martyniak²⁷, S. Masson², T. Mavroidis²⁰, S.J. Maxfield¹⁹, S.J. McMahon¹⁹, A. Mehta²²,
 K. Meier¹⁵, D. Mercer²², T. Merz³⁵, A. Meyer¹¹, C.A. Meyer³⁷, H. Meyer³⁴, J. Meyer¹¹,
 A. Migliori²⁸, S. Mikocki⁶, D. Milstead¹⁹, F. Moreau²⁸, J.V. Morris⁵, E. Mroczko⁶, G. Müller¹¹,
 K. Müller¹¹, P. Murín¹⁷, V. Nagovizin²⁴, R. Nahnauer³⁵, B. Naroska¹³, Th. Naumann³⁵,
 P.R. Newman³, D. Newton¹⁸, D. Neyret²⁹, H.K. Nguyen²⁹, T.C. Nicholls³, F. Niebergall¹³,
 C. Niebuhr¹¹, Ch. Niedzballa¹, R. Nisius¹, G. Nowak⁶, G.W. Noyes⁵, M. Nyberg-Werther²¹,
 M. Oakden¹⁹, H. Oberlack²⁶, U. Obrock⁸, J.E. Olsson¹¹, D. Ozerov²⁴, E. Panaro¹¹,

A. Panitch⁴, C. Pascaud²⁷, G.D. Patel¹⁹, E. Peppel³⁵, E. Perez⁹, J.P. Phillips²², Ch. Pichler¹², D. Pitzl³⁶, G. Pope⁷, S. Prell¹¹, R. Prosi¹¹, K. Rabbertz¹, G. Rädcl¹¹, F. Raupach¹, P. Reimer³⁰, S. Reinshagen¹¹, P. Ribarics²⁶, H.Rick⁸, V. Riech¹², J. Riedlberger³⁶, S. Riess¹³, M. Rietz², E. Rizvi²⁰, S.M. Robertson³, P. Robmann³⁷, H.E. Roloff³⁵, R. Roosen⁴, K. Rosenbauer¹, A. Rostovtsev²⁴, F. Rouse⁷, C. Royon⁹, K. Rüter²⁶, S. Rusakov²⁵, K. Rybicki⁶, R. Rylko²⁰, N. Sahlmann², D.P.C. Sankey⁵, P. Schacht²⁶, S. Schiek¹³, S. Schleif¹⁵, P. Schleper¹⁴, W. von Schlippe²⁰, D. Schmidt³⁴, G. Schmidt¹³, A. Schöning¹¹, V. Schröder¹¹, E. Schuhmann²⁶, B. Schwab¹⁴, G. Sciacca³⁵, F. Sefkow¹¹, M. Seidel¹², R. Sell¹¹, A. Semenov²⁴, V. Shekelyan¹¹, I. Sheviakov²⁵, L.N. Shtarkov²⁵, G. Siegmon¹⁶, U. Siewert¹⁶, Y. Sirois²⁸, I.O. Skillicorn¹⁰, P. Smirnov²⁵, J.R. Smith⁷, V. Solochenko²⁴, Y. Soloviev²⁵, J. Spiekermann⁸, S. Spielman²⁸, H. Spitzer¹³, R. Starosta¹, M. Steenbock¹³, P. Steffen¹¹, R. Steinberg², B. Stella³², K. Stephens²², J. Stier¹¹, J. Stiewe¹⁵, U. Stößlein³⁵, K. Stolze³⁵, J. Strachota³⁰, U. Straumann³⁷, W. Struczinski², J.P. Sutton³, S. Tapprogge¹⁵, V. Tchernyshov²⁴, C. Thiebaux²⁸, G. Thompson²⁰, P. Truöl³⁷, J. Turnau⁶, J. Tutas¹⁴, P. Uelkes², A. Usik²⁵, S. Valkár³¹, A. Valkárová³¹, C. Vallée²³, D. Vandenplas²⁸, P. Van Esch⁴, P. Van Mechelen⁴, A. Vartapetian^{11,38}, Y. Vazdik²⁵, P. Verrecchia⁹, G. Villet⁹, K. Wacker⁸, A. Wagener², M. Wagener³³, A. Walther⁸, G. Weber¹³, M. Weber¹¹, D. Wegener⁸, A. Wegner¹¹, H.P. Wellisch²⁶, L.R. West³, S. Willard⁷, M. Winde³⁵, G.-G. Winter¹¹, C. Wittek¹³, A.E. Wright²², E. Wünsch¹¹, N. Wulff¹¹, T.P. Yiou²⁹, J. Žáček³¹, D. Zarbock¹², Z. Zhang²⁷, A. Zhokin²⁴, M. Zimmer¹¹, W. Zimmermann¹¹, F. Zomer²⁷, K. Zuber¹⁵, and M. zurNedden³⁷

¹ *I. Physikalisches Institut der RWTH, Aachen, Germany^f*

² *III. Physikalisches Institut der RWTH, Aachen, Germany^f*

³ *School of Physics and Space Research, University of Birmingham, Birmingham, UK^b*

⁴ *Inter-University Institute for High Energies ULB-VUB, Brussels; Universitaire Instelling Antwerpen, Wilrijk, Belgium^c*

⁵ *Rutherford Appleton Laboratory, Chilton, Didcot, UK^b*

⁶ *Institute for Nuclear Physics, Cracow, Poland^d*

⁷ *Physics Department and IIRPA, University of California, Davis, California, USA^e*

⁸ *Institut für Physik, Universität Dortmund, Dortmund, Germany^f*

⁹ *CEA, DSM/DAPNIA, CE-Saclay, Gif-sur-Yvette, France*

¹⁰ *Department of Physics and Astronomy, University of Glasgow, Glasgow, UK^b*

¹¹ *DESY, Hamburg, Germany^f*

¹² *I. Institut für Experimentalphysik, Universität Hamburg, Hamburg, Germany^f*

¹³ *II. Institut für Experimentalphysik, Universität Hamburg, Hamburg, Germany^f*

¹⁴ *Physikalisches Institut, Universität Heidelberg, Heidelberg, Germany^f*

¹⁵ *Institut für Hochenergiephysik, Universität Heidelberg, Heidelberg, Germany^f*

¹⁶ *Institut für Reine und Angewandte Kernphysik, Universität Kiel, Kiel, Germany^f*

¹⁷ *Institute of Experimental Physics, Slovak Academy of Sciences, Košice, Slovak Republic^f*

¹⁸ *School of Physics and Chemistry, University of Lancaster, Lancaster, UK^b*

¹⁹ *Department of Physics, University of Liverpool, Liverpool, UK^b*

²⁰ *Queen Mary and Westfield College, London, UK^b*

²¹ *Physics Department, University of Lund, Lund, Sweden^g*

²² *Physics Department, University of Manchester, Manchester, UK^b*

²³ *CPPM, Université d'Aix-Marseille II, IN2P3-CNRS, Marseille, France*

²⁴ *Institute for Theoretical and Experimental Physics, Moscow, Russia*

²⁵ *Lebedev Physical Institute, Moscow, Russia^f*

- ²⁶ *Max-Planck-Institut für Physik, München, Germany^f*
- ²⁷ *LAL, Université de Paris-Sud, IN2P3-CNRS, Orsay, France*
- ²⁸ *LPNHE, Ecole Polytechnique, IN2P3-CNRS, Palaiseau, France*
- ²⁹ *LPNHE, Universités Paris VI and VII, IN2P3-CNRS, Paris, France*
- ³⁰ *Institute of Physics, Czech Academy of Sciences, Praha, Czech Republic^{f,h}*
- ³¹ *Nuclear Center, Charles University, Praha, Czech Republic^{f,h}*
- ³² *INFN Roma and Dipartimento di Fisica, Università "La Sapienza", Roma, Italy*
- ³³ *Paul Scherrer Institut, Villigen, Switzerland*
- ³⁴ *Fachbereich Physik, Bergische Universität Gesamthochschule Wuppertal, Wuppertal, Germany^f*
- ³⁵ *DESY, Institut für Hochenergiephysik, Zeuthen, Germany^f*
- ³⁶ *Institut für Teilchenphysik, ETH, Zürich, Switzerlandⁱ*
- ³⁷ *Physik-Institut der Universität Zürich, Zürich, Switzerlandⁱ*
- ³⁸ *Visitor from Yerevan Phys.Inst., Armenia*

^a *Supported by the Bundesministerium für Forschung und Technologie, FRG under contract numbers 6AC17P, 6AC47P, 6DO57I, 6HH17P, 6HH27I, 6HD17I, 6HD27I, 6KI17P, 6MP17I, and 6WT87P*

^b *Supported by the UK Particle Physics and Astronomy Research Council, and formerly by the UK Science and Engineering Research Council*

^c *Supported by FNRS-NFWO, IISN-IIKW*

^d *Supported by the Polish State Committee for Scientific Research, grant No. 204209101*

^e *Supported in part by USDOE grant DE F603 91ER40674*

^f *Supported by the Deutsche Forschungsgemeinschaft*

^g *Supported by the Swedish Natural Science Research Council*

^h *Supported by GA ČR, grant no. 202/93/2423, GA AV ČR, grant no. 19095 and GA UK, grant no. 342*

ⁱ *Supported by the Swiss National Science Foundation*

1 Introduction

The $e^\pm p$ collider HERA, in which 27.5 GeV (26.7 GeV in 1993) leptons collide with 820 GeV protons, provides access to an as yet unexplored mass domain for the discovery of new particles. Several extensions of the Standard Model postulate either new fermions or new bosons, such as leptoquarks and additional gauge bosons. Signals for physics beyond the Standard Model can be discovered either directly or indirectly.

Common to all *direct* searches is the s channel formation of a new heavy resonance at a mass $M_X = \sqrt{x s}$, which is, however, limited by the available centre of mass energy of $\sqrt{s} \simeq 300$ GeV. The scaling variable x is the momentum fraction of the proton carried by the struck quark. Results of direct searches for new heavy bosons at HERA have been published recently by the experiments H1 [1] and ZEUS [2].

The search for new bosons or $e q$ compositeness can be considerably extended beyond the kinematic production limit through the study of *indirect* effects from virtual particle exchange. Such effects may become observable as deviations from the Standard Model expectation at high momentum transfers Q^2 .

The analysis presented here combines all data collected with the H1 experiment at HERA during 1993 and 1994 with electron and positron beams. They represent an increase in integrated luminosity by a factor of ~ 9 compared to the previous data sample [1].

2 Phenomenology of $(\bar{e} e) (\bar{q} q)$ Contact Interactions

New currents or bosons may produce indirect effects through the interference of a *virtual* particle exchange with the γ and Z fields of the Standard Model. For particle masses well above the available production energy, such indirect signatures may be investigated by adding general contact interaction terms to the Standard Model Lagrangian. Sufficiently heavy particles X cease to propagate and thus new contact terms and modified vertices arise from ‘contracting’ the particle propagators to an effective 4-fermion point-like interaction. The separate dependence of s , t and u channel amplitudes on couplings $g_{X \rightarrow i, f}$ to states i , f and mass M_X reduce to the dependence on effective couplings with dimension [mass $^{-2}$]

$$\eta_{if} \equiv \frac{g_{X \rightarrow i} g_{X \rightarrow f}}{M_X^2} .$$

The most general chiral invariant neutral current contact interaction Lagrangian can be written in the form [3]

$$\begin{aligned} \mathcal{L}_{\text{contact}}^{NC} = & \sum_{q=u,d} \{ \eta_{LL}^q (\bar{e}_L \gamma_\mu e_L) (\bar{q}_L \gamma^\mu q_L) + \eta_{LR}^q (\bar{e}_L \gamma_\mu e_L) (\bar{q}_R \gamma^\mu q_R) \\ & + \eta_{RL}^q (\bar{e}_R \gamma_\mu e_R) (\bar{q}_L \gamma^\mu q_L) + \eta_{RR}^q (\bar{e}_R \gamma_\mu e_R) (\bar{q}_R \gamma^\mu q_R) \} , \end{aligned}$$

where the indices L and R denote the left-handed and right-handed fermion helicities and the sum extends over *up* and *down* quarks and antiquarks q .

Although contact interactions have been originally proposed in the context of composite leptons and quarks [4, 5], this ansatz can be easily applied to other new phenomena [3] by an appropriate choice of the coupling coefficients η_{if} .

Leptoquarks are colour triplet bosons of spin 0 or 1, carrying lepton (L) and baryon (B) number and fractional electric charge. They couple to lepton-quark pairs and appear in almost

all extensions of the Standard Model which try to establish a connection between leptons and quarks [6, 7]. Leptons and quarks may be either arranged in common multiplets, like in Grand Unified Theories or superstring motivated E_6 models, or they may have a common substructure as in composite models. A fermion number $F = L + 3B$ is defined, which takes the values $F = 2$ for leptoquarks coupling to $e^- q$ and $F = 0$ for leptoquarks coupling to $e^- \bar{q}$. For positrons the fermion number F changes by two units. Consequently $F = 2$ leptoquarks are easier accessible in $e^- p$ scattering, while positron beams are more sensitive to $F = 0$ leptoquarks, since at moderate x values quarks are more abundant in the proton than antiquarks.

The notation, the contact interaction coefficients η_{if} and the fermion number assignment for leptoquarks with mass M_{LQ} and coupling λ are given in Table 2 (from ref. [3]). The only unknown is the ratio M_{LQ}/λ . Note that vector leptoquarks have positive coupling coefficients, while scalar leptoquarks have negative coupling coefficients, being a factor of 2 smaller in magnitude.

In the Standard Model the fundamental particles – leptons, quarks and gauge bosons – are assumed to be pointlike. A possible fermion **compositeness** or substructure can be expressed through $\eta_{if} \equiv \pm g^2/\Lambda_{if}^{\pm 2}$, where the signs indicate positive and negative interference with the Standard Model currents, g is the coupling strength conventionally chosen as $g^2/4\pi = 1$ and Λ is the compositeness scale.

3 The H1 Detector

A detailed description of the H1 detector can be found elsewhere [8]. Here only those components are described, which are relevant for the present analysis.

The lepton energy and angle is measured in a finely segmented liquid argon (LAr) sampling calorimeter covering the polar angle¹ range $4^\circ \leq \theta \leq 153^\circ$ and all azimuthal angles. It consists of a lead/argon electromagnetic section with a thickness varying between 20 and 30 radiation lengths and a stainless steel/argon section for the measurement of hadronic energy flow, which offers in total a containment varying from 4.5 up to 8 interaction lengths. Electron energies are measured with a resolution of $\sigma(E)/E \simeq 12\%/\sqrt{E} \oplus 1\%$ and hadron energies with $\sigma(E)/E \simeq 50\%/\sqrt{E} \oplus 2\%$. The absolute energy scales are known to 3% and 5% for electrons and hadrons, respectively. The angular resolution of the scattered lepton measured from the electromagnetic shower in the calorimeter is ~ 7 mrad. A lead/scintillator electromagnetic backward calorimeter extends the coverage at large angles ($155^\circ \leq \theta \leq 176^\circ$). The instrumented iron flux return yoke is used to measure the leakage of hadronic showers.

Located inside the calorimeters is a tracking system, which consists of central drift and proportional chambers ($25^\circ \leq \theta \leq 155^\circ$), a forward track detector ($7^\circ \leq \theta \leq 25^\circ$) and backward proportional chambers ($155^\circ \leq \theta \leq 175^\circ$). The tracking chambers and calorimeters are surrounded by a superconducting solenoid coil providing a uniform field of 1.15 T within the tracking volume.

The luminosity is determined from the rate of the Bethe–Heitler process $ep \rightarrow ep\gamma$ measured in a luminosity monitor [9] far downstream the electron direction. The systematic errors of the integrated luminosity vary between 1.8% (1994 data) and 4.5% (1993 data).

¹The incoming proton moves in the $+z$ direction with polar angle $\theta = 0^\circ$.

4 Data Selection and Analysis

The analysis is based on a purely inclusive measurement of the final state lepton in deep inelastic neutral current events $e^\pm p \rightarrow e^\pm \text{hadrons}$. All quantities of event properties are determined from the calorimeters alone, tracking information is only used to get the primary vertex position. The kinematic variables Q^2 , the negative squared momentum transfer, and the scaling variable y are derived from the scattered lepton energy E'_e and polar angle θ_e

$$Q^2 = 4 E_e E'_e \cos^2 \frac{\theta_e}{2},$$

$$y = 1 - \frac{E'_e}{E_e} \sin^2 \frac{\theta_e}{2},$$

where E_e is the lepton beam energy. These quantities are related to the Bjorken scaling variable x by $Q^2 = x y s$.

The data were taken in three periods: (i) during 1993 with 26.7 GeV electrons, (ii) during 1994 with 27.5 GeV electrons, and (iii) during 1994 with 27.5 GeV positrons. The event selection is similar to the previous leptoquark analysis [1] with the following requirements:

1. The transverse energy of the scattered lepton has to exceed $E'_{\perp,e} > 8$ GeV.
2. The polar angle of the scattered lepton has to be within the LAr calorimeter acceptance $10^\circ < \theta_e < 150^\circ$.
3. A primary vertex has to be reconstructed within $|z_{vertex} - \langle z \rangle| < 35$ cm of the nominal interaction point $\langle z \rangle$.
4. The energy–longitudinal momentum conservation $|\sum (E - p_z) - 2 E_e| < 10$ GeV must be satisfied, where the sum extends over all detected particles or energy clusters.
5. The event has to be balanced in transverse momentum $|\vec{p}_\perp^{evt}| < 15$ GeV.
6. The scaling variable y has to fulfill $y < 0.8$.

Requirements (1) and (2) assure that the kinematic quantities are well measured in the LAr calorimeter. Q^2 is always well measured, while the resolution in y degrades at low values of $y \lesssim 0.1$. The requirements (3) and (5) suppress beam–wall and beam–gas background. The criteria (4) and (5) provide a good containment of the final state particles and reject events with a hard photon radiated from the initial state lepton and photoproduction events with a misidentified lepton in the LAr calorimeter. For events with all final state particles detected (except the proton remnants) one expects $\sum (E - p_z) \approx 2 E_e$. Requirement (6) is introduced to avoid the region affected by large radiative corrections and to suppress photoproduction events with a misidentified lepton. The remaining contamination from photoproduction, beam–gas collisions and cosmic rays is negligible.

The final data samples consist of (i) 739 events for an integrated luminosity of $\mathcal{L} = 0.418 (\pm 4.5\%) \text{ pb}^{-1}$ of the $e^- p$ 1993 data, (ii) 810 events for $\mathcal{L} = 0.491 (\pm 2.4\%) \text{ pb}^{-1}$ of the $e^- p$ 1994 data, and (iii) 5201 events for $\mathcal{L} = 2.947 (\pm 1.8\%) \text{ pb}^{-1}$ of the $e^+ p$ 1994 data.

The measured cross sections $d\sigma/dQ^2$ are corrected for detector effects and QED radiation and extrapolated to the full kinematic phase space. The correction factors for each Q^2 bin are

obtained from Monte Carlo studies. Deep inelastic scattering events are generated according to the Standard Model cross section

$$\frac{d^2\sigma(e^\pm p \rightarrow e^\pm X)}{dx dQ^2} = \frac{2\pi\alpha^2}{xQ^4} \left\{ Y_+ F_2(x, Q^2) - y^2 F_L(x, Q^2) \mp Y_- x F_3(x, Q^2) \right\},$$

$$Y_\pm = 1 \pm (1 - y)^2$$

using the parton densities from the MRS H parametrization [10] of the structure functions $F_i(x, Q^2)$. The longitudinal structure function F_L has not yet been measured at HERA, but is expected to give very small contributions only at low Q^2 and low x values. For the present analysis F_L has been neglected. Radiative effects are taken into account by the event generator DJANGO 6 [11], which includes the $\mathcal{O}(\alpha)$ electroweak corrections and the QCD matrix elements to first order in α_s , supplemented by leading-logarithmic parton showers. The lepton detection and measurement is simulated by smearing the event vertex and the generated four-vector according to measured resolutions, acceptances and efficiencies, as determined from data. The hadron final state is simulated by smearing the four-vector of the ‘struck quark’ as calculated from the electron kinematics (no hadronization). This very fast and efficient acceptance simulation is completely adequate to describe all properties of the deep inelastic scattering events used in the present inclusive analysis.

5 Results

Cross Sections

The corrected differential cross sections $d\sigma/dQ^2$ for the $e^- p$ and $e^+ p$ data are shown in Fig. 1 and listed in Table 1. Statistical and systematic errors are added in quadrature, except for an overall normalization uncertainty. The systematic errors include uncertainties of the trigger and detection efficiencies, the vertex reconstruction and the lepton energy calibration of the LAr calorimeter (all determined from the data), as well as uncertainties due to radiative corrections and the choice of different parton distributions (MRS H, MRS D⁰ and MRS D⁻). The systematic uncertainties are typically $\sim 2\%$, except for the energy calibration, which contributes $\sim 6\%$ in the low Q^2 region. The overall normalization errors are 3.5% for the $e^- p$ data and 1.8% for the $e^+ p$ data and account for uncertainties of the luminosity measurement. The acceptance is a smooth function of the squared momentum transfer. It rises from $\sim 65\%$ at the lowest Q^2 to $\sim 80\%$ at $Q^2 \simeq 1000 \text{ GeV}^2$ and then slowly decreases to $\sim 60\%$ at $Q^2 \simeq 10,000 \text{ GeV}^2$. The extrapolation to the full phase space is not critical for the low and medium Q^2 region, where the validity of the Standard Model is well established. At high Q^2 and large y the Standard Model is assumed. The effects of the extrapolation on the contact interaction analysis are, however, small.

The measured cross sections are well described by the Standard Model expectations over five orders of magnitude in the Q^2 range between 160 GeV^2 and 20,000 GeV^2 . No significant deviation is observed for either lepton charge, see Fig. 1.

It is interesting to note that the $e^- p$ cross section tends to be slightly higher than the $e^+ p$ cross section at high Q^2 values, as expected from the different couplings of the leptons to the Z boson. The charge asymmetry is, however, not yet significant due to the limited electron data statistics.

The contact interaction analysis investigates the differential cross sections $d\sigma/dQ^2$ and interpretes any deviation from the Standard Model as lower limits on the ratio mass over coupling

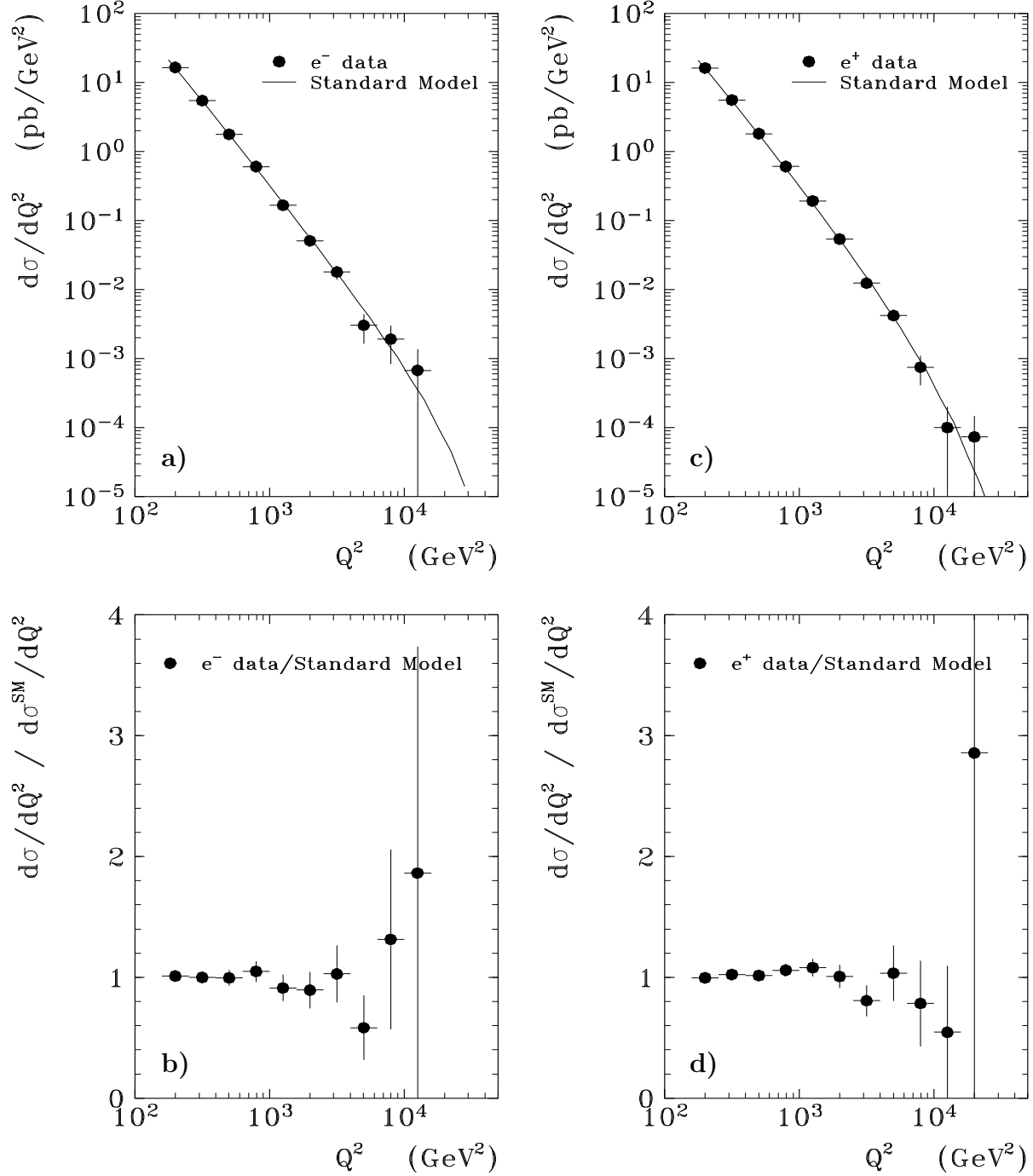


Figure 1: Differential cross sections $d\sigma/dQ^2$ versus Q^2 (\bullet) in comparison with the Standard Model expectations ($—$). **a)** and **b)** $e^- p$ data, **c)** and **d)** $e^+ p$ data. The error bars represent statistical and systematic errors added in quadrature, except for an overall normalization uncertainty of 3.5% ($e^- p$ data) and 1.8% ($e^+ p$ data), respectively.

$\langle Q^2 \rangle$ [GeV ²]	$e^- p$ data	$e^+ p$ data
	$d\sigma/dQ^2$ [pb GeV ⁻²]	$d\sigma/dQ^2$ [pb GeV ⁻²]
200	$16.5 \pm 0.7 \pm 0.6$	$16.2 \pm 0.4 \pm 0.8$
316	$5.43 \pm 0.25 \pm 0.11$	$5.57 \pm 0.14 \pm 0.16$
501	$1.77 \pm 0.11 \pm 0.04$	$1.81 \pm 0.06 \pm 0.06$
794	$(6.03 \pm 0.48 \pm 0.11) \cdot 10^{-1}$	$(6.04 \pm 0.27 \pm 0.15) \cdot 10^{-1}$
1259	$(1.66 \pm 0.19 \pm 0.05) \cdot 10^{-1}$	$(1.92 \pm 0.12 \pm 0.06) \cdot 10^{-1}$
1995	$(5.09 \pm 0.84 \pm 0.21) \cdot 10^{-2}$	$(5.38 \pm 0.49 \pm 0.13) \cdot 10^{-2}$
3162	$(1.79 \pm 0.40 \pm 0.09) \cdot 10^{-2}$	$(1.23 \pm 0.19 \pm 0.04) \cdot 10^{-2}$
5012	$(3.02 \pm 1.14 \pm 0.77) \cdot 10^{-3}$	$(4.19 \pm 0.91 \pm 0.18) \cdot 10^{-3}$
7943	$(1.91 \pm 0.95 \pm 0.51) \cdot 10^{-3}$	$(7.50 \pm 3.36 \pm 0.48) \cdot 10^{-4}$
12589	$(6.74 \pm 6.74 \pm 0.66) \cdot 10^{-4}$	$(1.00 \pm 1.00 \pm 0.11) \cdot 10^{-4}$
19953	—	$(7.32 \pm 7.32 \pm 1.49) \cdot 10^{-5}$

Table 1: Differential cross sections $d\sigma/dQ^2$ for the $e^- p$ and $e^+ p$ data with statistical and systematic errors. There is an additional overall normalization uncertainty of 3.5% ($e^- p$ data) and 1.8% ($e^+ p$ data), respectively, due to systematic errors of the luminosity measurement.

strength of new heavy leptoquarks or composite eq structures. It is assumed that possible deviations are caused by only one new boson exchange at the time. A combined χ^2 analysis of the $e^- p$ and $e^+ p$ data is performed including for each data set an individual overall normalization constant f_{norm} with its corresponding error Δ_{norm} (see discussion above)

$$\chi^2 = \sum_{l=e^-, e^+} \left\{ \sum_k \left(\frac{\sigma_k^l(Q^2) f_{norm}^l - \sigma^{theor}(Q^2, \eta_{if})}{\Delta\sigma_k^l(Q^2) f_{norm}^l} \right)^2 + \left(\frac{f_{norm}^l - 1}{\Delta_{norm}^l} \right)^2 \right\}.$$

The inner sum extends over the bins of one data set, while the outer sum is taken over both the $e^- p$ and $e^+ p$ data. Thus, fitted parameters are the η_{if} coefficients of the contact interaction model and the two normalization constants. Limits at 95% confidence level are derived from the increase of χ^2 by 3.89 with respect to its minimum value, which in most cases coincides with the Standard Model fit. Enlarging the normalization errors arbitrarily by 2% would lower the resulting limits by $\sim 5\%$. Choosing different parton distributions, MRS D^{0'} or MRS D^{-'}, in the cross section calculation changes the limits by $\sim 3\%$ in either direction.

Leptoquarks

The results of the leptoquark analysis are summarized in Table 2. Only those lower limits on M_{LQ}/λ are quoted, which exceed the kinematic phase space of HERA for direct production assuming a strong coupling of $\lambda = 1$.

One notices that vector leptoquarks with a positive coupling to u quarks provide the most restrictive bounds approaching $\mathcal{O}(1 \text{ TeV})$. The sensitivity to scalar leptoquarks is generally lower by a factor of ~ 2 and two of them, \tilde{S}_0^R and $\tilde{S}_{1/2}^L$, have only couplings to d quarks. It is not obvious which leptoquarks will provide the most stringent limits, when arguing alone on the basis of the assigned fermion numbers F and quark densities in the proton. In addition to the s channel amplitudes of direct production the contact interaction ansatz implicitly contains the

leptoquark	coupling to u quark [GeV ⁻²]	coupling to d quark [GeV ⁻²]	F	M_{LQ}/λ [GeV]
S_0^L	$\eta_{LL}^u = -\frac{1}{2} (\lambda/M_{LQ})^2$		2	
S_0^R	$\eta_{RR}^u = -\frac{1}{2} (\lambda/M_{LQ})^2$		2	
\tilde{S}_0^R		$\eta_{RR}^d = -\frac{1}{2} (\lambda/M_{LQ})^2$	2	350
$S_{1/2}^L$	$\eta_{LR}^u = -\frac{1}{2} (\lambda/M_{LQ})^2$		0	
$S_{1/2}^R$	$\eta_{RL}^u = -\frac{1}{2} (\lambda/M_{LQ})^2$	$\eta_{RL}^d = -\frac{1}{2} (\lambda/M_{LQ})^2$	0	
$\tilde{S}_{1/2}^L$		$\eta_{LR}^d = -\frac{1}{2} (\lambda/M_{LQ})^2$	0	360
S_1^L	$\eta_{LL}^u = -\frac{1}{2} (\lambda/M_{LQ})^2$	$\eta_{LL}^d = -1 (\lambda/M_{LQ})^2$	2	340
V_0^L		$\eta_{LL}^d = +1 (\lambda/M_{LQ})^2$	0	
V_0^R		$\eta_{RR}^d = +1 (\lambda/M_{LQ})^2$	0	
\tilde{V}_0^R	$\eta_{RR}^u = +1 (\lambda/M_{LQ})^2$		0	760
$V_{1/2}^L$		$\eta_{LR}^d = +1 (\lambda/M_{LQ})^2$	2	300
$V_{1/2}^R$	$\eta_{RL}^u = +1 (\lambda/M_{LQ})^2$	$\eta_{RL}^d = +1 (\lambda/M_{LQ})^2$	2	710
$\tilde{V}_{1/2}^L$	$\eta_{LR}^u = +1 (\lambda/M_{LQ})^2$		2	800
V_1^L	$\eta_{LL}^u = +2 (\lambda/M_{LQ})^2$	$\eta_{LL}^d = +1 (\lambda/M_{LQ})^2$	0	1020

Table 2: Contact interaction coefficients η_{if}^q , fermion number F and lower limits at 95% confidence level on M_{LQ}/λ for scalar (S) and vector (V) leptoquarks. The leptoquark notation indicates the lepton chirality L, R and the weak isospin $I = 0, 1/2, 1$. The leptoquarks \tilde{S} and \tilde{V} differ by two units of hypercharge from S and V , respectively.

crossed t and u channel diagrams. Moreover, not all coupling coefficients η_{if} contribute with the same weight, thus spoiling the naive expectation².

As an illustration of the sensitivity of the data to virtual leptoquark exchange Fig. 2 shows the allowed contribution of a vector leptoquark V_1^L . The contact interaction contributions to the Standard Model rise with Q^2 as expected and amount to $\sim 25\%$ at the highest Q^2 values.

The *indirect* limits M_{LQ}/λ derived from virtual leptoquark exchange nicely complement the *direct* searches [1, 2], because they exceed the kinematic range of HERA at large couplings. The couplings λ can be safely extracted down to the nominal centre of mass energy, since the present integrated luminosities restrict the accessible masses to $M_{LQ} = \sqrt{x s} \lesssim 250$ GeV. For example, a vector leptoquark V_1^L with a mass of 300 GeV can be excluded for couplings larger than the electromagnetic strength $\lambda > \sqrt{4\pi\alpha} = 0.3$.

The limits given in Table 2 can be compared to those derived from other, primarily low energy experiments. The strongest bounds for leptoquarks coupling to the first lepton and quark generations arise from atomic parity violation experiments and from universality in leptonic π decays. Davidson *et al.* [12] give M_{LQ}/λ limits in the range of 1.6 to 2.2 TeV for scalar leptoquarks and 2.2 to 3.1 TeV for vector leptoquarks, while Leurer [13] arrives at values up to a factor of ~ 1.5 either lower or higher, and generally gets larger values for scalar than for vector leptoquarks. Despite of these uncertainties, our most stringent limits for vector

²A comprehensive general discussion on the sensitivity of the coupling coefficients in the eight-dimensional η_{if} space can be found in ref. [3].

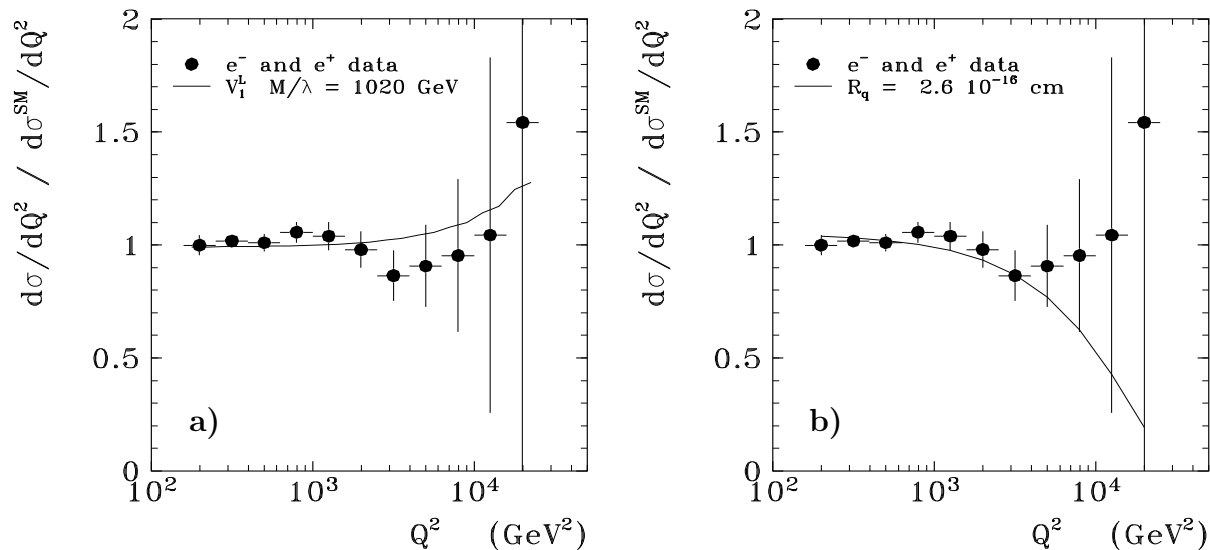


Figure 2: Differential cross sections $d\sigma/dQ^2$ normalized to the Standard Model expectation versus Q^2 for the combined $e^- p$ and $e^+ p$ data (\bullet). The error bars represent statistical and systematic errors added in quadrature, but do not contain an overall luminosity uncertainty (see text). **a)** The curve shows the allowed contribution (95% confidence level) of a vector leptoquark V_1^L with $M_{LQ}/\lambda = 1020$ GeV. **b)** The curve shows the effect of a form factor with a quark radius $R_q = 2.6 \cdot 10^{-16}$ cm (95% confidence level).

leptoquarks are within a factor of two close to the ones extracted from the very low energy experiments. They provide, however, very useful complementary information at much higher momentum transfers from a model independent analysis involving no theoretical assumptions on higher order corrections.

Compositeness Scales

If quarks and leptons have a substructure and have common constituents they may form composite objects. Such virtual states are characterized by a compositeness scale parameter Λ and a coupling strength g , which is set to $g^2/4\pi = 1$ in the present analysis.

The results for lower limits on the eq compositeness scale parameters Λ^\pm are summarized in Table 3. They vary between 1.0 TeV and 2.5 TeV, depending on the chiral structure and the sign of interference with the Standard Model currents. The bounds with positive interference are more stringent than those with negative interference. There is almost no difference between various lepton and quark chiralities.

Λ_{LL}^+	Λ_{LL}^-	Λ_{LR}^+	Λ_{LR}^-	Λ_{RL}^+	Λ_{RL}^-	Λ_{RR}^+	Λ_{RR}^-
2.3	1.0	2.5	1.2	2.5	1.2	2.3	1.0

Table 3: Lower limits at 95% confidence level on compositeness scale parameters Λ^\pm [TeV] for chiralities LL , LR , RL and RR with positive and negative interference with the Standard Model currents. The coupling constants are $\pm g^2/\Lambda^{\pm 2}$ with the convention $g^2/4\pi = 1$.

Although it is common practice to give bounds on Λ^\pm , it is more appropriate to fit directly $\eta_{if} = g^2/\Lambda_{if}^2$ as used in the contact interaction Lagrangian. This has the advantage that the errors behave rather gaussian. Limits on Λ^\pm for a certain interference are then derived from the corresponding upper and lower values of $1/\Lambda^2$ at a given confidence level. A fit of $1/\Lambda^2$ yields $\Lambda_{LL}^{-2} = \Lambda_{RR}^{-2} = (-0.41 \pm 0.33) \text{ TeV}^{-2}$ and $\Lambda_{LR}^{-2} = \Lambda_{RL}^{-2} = (-0.30 \pm 0.23) \text{ TeV}^{-2}$, assuming a coupling strength of $g^2/4\pi = 1$.

The compositeness scale parameters Λ can be interpreted in terms of a radius of the $e q$ system via $R_{eq} = \sqrt{4\pi/g'^2} \Lambda^{-1}$. Depending on the chiral structure and the sign of interference the size of a composite $e q$ state is constrained to $R_{eq} \lesssim (0.8 \div 2) \cdot 10^{-17} \text{ cm}$, if a strong coupling strength g' is assumed.

Our limits on Λ^\pm are comparable to those derived in similar studies at $p\bar{p}$ and e^+e^- colliders [14]. For example CDF quotes $\Lambda_{LL}^+ > 1.7 \text{ TeV}$ and $\Lambda_{LL}^- > 2.2 \text{ TeV}$ for the light u and d quarks and VENUS quotes $\Lambda_{LL}^+ > 1.2 \text{ TeV}$ and $\Lambda_{LL}^- > 1.6 \text{ TeV}$ assuming flavour universality for five quarks.

Form Factors

An alternative method to study possible fermion substructures is to assign a finite size of radius R to the leptons and/or quarks [15]. A convenient parametrization is to introduce in a ‘classical’ way form factors $f(Q^2)$ at the gauge boson–fermion vertices, which depend on the squared momentum transfer Q^2

$$f(Q^2) = 1 - \frac{1}{6} R^2 Q^2 .$$

For simplicity, the radius R is assumed to be universal for the electromagnetic and the weak vector and axial-vector fermion couplings. The form factors reduce to unity and the couplings to the familiar Standard Model values in the pointlike limit. A finite extension of a lepton or quark is expected to diminish the Standard Model cross section at high Q^2 according to

$$\frac{d\sigma}{dQ^2} = \frac{d\sigma^{SM}}{dQ^2} f_e^2(Q^2) f_q^2(Q^2) .$$

The data are analyzed in terms of a single form factor, yielding as an upper limit at 95% confidence level a radius of

$$R < 2.6 \cdot 10^{-16} \text{ cm} .$$

This result may be interpreted as a limit on the light quark sizes, since the pointlike nature of the electron is already established down to much lower distances in e^+e^- and $(g-2)_e$ experiments [16]. Fig 2 b shows the effect of a form factor with a quark radius R_q given by the experimental limit on the differential cross sections; again the sensitivity rises with Q^2 .

The limit on R_q is within a factor of two comparable to the bounds derived from a global analysis of Z decays at LEP [15].

Similar upper limits on a quark radius (up to a factor of $\sqrt{6}$) are obtained from the above contact term analysis, if the compositeness scale parameters Λ^- are evaluated at the electromagnetic scale $g^2/4\pi = \alpha$. Note, however, that in this interpretation the size is inferred from the interference of the Standard Model currents with a new virtual current.

6 Conclusions

An analysis of searches for new phenomena beyond the Standard Model mediated through contact interactions in deep inelastic scattering at HERA has been presented. The data correspond to a 9 fold increase in integrated luminosity compared to a previous publication [1].

The differential cross sections $d\sigma/dQ^2$ have been measured for deep inelastic neutral current $e^\pm p$ scattering in the Q^2 range between 160 GeV² and 20,000 GeV². No significant deviations from the Standard Model have been observed for either lepton charge.

Substantially improved limits at 95% confidence level on masses and couplings of new heavy leptoquarks and on fermion compositeness scales have been obtained, using the combined $e^- p$ and $e^+ p$ cross section data.

Eight out of fourteen possible leptoquark couplings yield lower limits on M_{LQ}/λ which exceed the centre of mass energy of HERA, assuming a strong coupling $\lambda = 1$, and therefore nicely complement the searches for direct production. Vector leptoquarks yield stronger limits than scalar leptoquarks and approach bounds on M_{LQ}/λ of 1 TeV.

A conceivable eq compositeness or fermion substructure can be ruled out for scale parameters Λ^\pm smaller than 1.0 TeV to 2.5 TeV, depending on the assumed fermion chiralities and the sign of interference with the Standard Model currents.

Finally, a form factor analysis constrains the size of the light u and d quarks to radii smaller than $R_q < 2.6 \cdot 10^{-16}$ cm.

The contact interaction concept has been shown to be a very powerful tool, becoming even more important in future high statistics data analyses. The sensitivity to new virtual boson exchanges roughly scales as $(\mathcal{L} s)^{\frac{1}{4}}$ with integrated luminosity \mathcal{L} and centre of mass energy squared s .

Acknowledgements. We are grateful to the HERA machine group, whose outstanding efforts made this experiment possible. We appreciate the immense contributions of the engineers and technicians, who constructed and maintained the detector. We thank the funding agencies for financial support. We acknowledge the support of the DESY technical staff. We also wish to thank the DESY directorate for the hospitality extended to the non-DESY members of the H1 collaboration.

References

- [1] H1 Collaboration, T. Ahmed *et al.*, Z. Phys. C64 (1994) 545.
- [2] ZEUS Collaboration, M. Derrick *et al.*, Phys. Lett. B306 (1993) 173.
- [3] P. Haberl, F. Schrempp and H.-U. Martyn, Proc. Workshop ‘*Physics at HERA*’, eds. W. Buchmüller and G. Ingelman, DESY, Hamburg (1991), vol. 2, p. 1133.
- [4] E. Eichten, K. Lane and M.E. Peskin, Phys. Rev. Lett. 50 (1983) 811.
- [5] R. Rückl, Phys. Lett. 120B (1983) 363; Nucl. Phys. B234 (1984) 91.
- [6] W. Buchmüller, R. Rückl and D. Wyler, Phys. Lett. B191 (1987) 442.
- [7] B. Schrempp, Proc. Workshop ‘*Physics at HERA*’, eds. W. Buchmüller and G. Ingelman, DESY, Hamburg (1991), vol. 2, p. 1034.
- [8] H1 Collaboration, I. Abt *et al.*, ‘*The H1 Detector at HERA*’, DESY 93-103 (1993).
- [9] H1 Collaboration, T. Ahmed *et al.*, Phys. Lett. B299 (1993) 374.
- [10] A.D. Martin, W.J. Stirling and R.G. Roberts, Phys. Lett. B306 (1993) 145; *ibid.* B309 (1993) 492.
- [11] G. A. Schuler and H. Spiessberger, Proc. Workshop ‘*Physics at HERA*’, eds. W. Buchmüller and G. Ingelman, DESY, Hamburg (1991), vol. 3, p. 1419.
- [12] S. Davidson, D. Baily and B. Campbell, Z. Phys. C61 (1994) 613.
- [13] M. Leurer, Phys. Rev. D49 (1994) 333; *ibid.* D50 (1994) 536.
- [14] Particle Data Group, Phys. Rev. D50 (1994) 1173.
- [15] G. Köpp, D. Schaile, M. Spira and P. Zerwas, DESY 94-148 (1994).
- [16] see e.g. reviews by T. Kinoshita and D.R. Yennie, H.-U. Martyn, and R.S. van Dyck Jr. in ‘*Quantum Electrodynamics*’, ed. T. Kinoshita, World Scientific (1990).